Regularity criterion for solutions of the three-dimensional Cahn-Hilliard-Navier-Stokes equations and associated computations

John D. Gibbon,[1] Nairita Pal,[2] Anupam Gupta,[3] and Rahul Pandit[2]

[1]*Department of Mathematics, Imperial College London, London SW7 2AZ, United Kingdom*
[2]*Centre for Condensed Matter Theory, Department of Physics, Indian Institute of Science, Bangalore, 560 012, India*
[3]*Department of Physics, University of Rome 'Tor Vergata', 00133 Rome, Italy*

We consider the three-dimensional (3D) Cahn-Hilliard equations coupled to, and driven by, the forced, incompressible 3D Navier-Stokes equations. The combination, known as the Cahn-Hilliard-Navier-Stokes (CHNS) equations, is used in statistical mechanics to model the motion of a binary fluid. The potential development of singularities (blow-up) in the contours of the order parameter ϕ is an open problem. To address this we have proved a theorem that closely mimics the Beale-Kato-Majda theorem for the 3D incompressible Euler equations [J. T. Beale, T. Kato, and A. J. Majda, Commun. Math. Phys. **94**, 61 (1984)]. By taking an L^∞ norm of the energy of the full binary system, designated as E_∞, we have shown that $\int_0^t E_\infty(\tau)\,d\tau$ governs the regularity of solutions of the full 3D system. Our direct numerical simulations (DNSs) of the 3D CHNS equations for (a) a gravity-driven Rayleigh Taylor instability and (b) a constant-energy-injection forcing, with 128^3 to 512^3 collocation points and over the duration of our DNSs confirm that E_∞ remains bounded as far as our computations allow.

I. INTRODUCTION

The Navier-Stokes (NS) equations [1–6], the fundamental partial differential equations (PDEs) that govern viscous fluid dynamics, date back to 1822. Since its introduction in 1958 the Cahn-Hilliard (CH) PDE [7], the fundamental equation for the statistical mechanics of binary mixtures, has been used extensively in studies of critical phenomena, phase transitions [8–13], nucleation [14], spinodal decomposition [15–19], and the late stages of phase separation [19,20]. If the two components of the binary mixture are fluids, the CH and NS equations must be coupled, where the resulting system of PDEs is usually referred to as model H [9] or the Cahn-Hilliard-Navier-Stokes (CHNS) equations.

The increasing growth of interest in the CHNS equations arises from the elegant way in which they allow us to follow the spatiotemporal evolution of the two fluids in the mixture *and the interfaces between them*. These interfaces are diffuse, so we do not have to impose boundary conditions on the moving boundaries between two different fluids, as in other methods for the simulation of multiphase flows [12,21,22]. However, in addition to a velocity field $\boldsymbol{u}$, we must also follow the scalar, order-parameter field ϕ, which distinguishes the two phases in a binary-fluid mixture. Here, interfacial regions are characterized by large gradients in ϕ. The CHNS equations have been used to model many binary-fluid systems that are of great current interest; examples include studies of (a) the Rayleigh-Taylor instability [23,24], (b) turbulence-induced suppression of the phase separation of the two components of the binary fluid [17], (c) multifractal droplet dynamics in a turbulent, binary-fluid mixture [25], (d) the coalescence of droplets [26], and (e) lattice-Boltzmann treatments of multiphase flows [17,27].

The system of CHNS equations is written as follows [24,28–30]:

$$(\partial_t + \boldsymbol{u}\cdot\boldsymbol{\nabla})\boldsymbol{u} = -\boldsymbol{\nabla}P/\rho + \nu\nabla^2\boldsymbol{u} - \alpha\boldsymbol{u} - (\phi\boldsymbol{\nabla}\mu) - A\boldsymbol{g} + \boldsymbol{f}, \quad (1)$$

$$(\partial_t + \boldsymbol{u}\cdot\boldsymbol{\nabla})\phi = \gamma\nabla^2\mu, \quad (2)$$

where P is pressure and $\rho\,(=1)$ is the constant density, together with the incompressibility condition $\boldsymbol{\nabla}\cdot\boldsymbol{u}=0$. In Eq. (1), $\boldsymbol{u}\equiv(u_x,u_y,u_z)$ is the fluid velocity and ν is the kinematic viscosity. In the two-dimensional (2D) case, $u_z=0$ and the air-drag-induced friction α should be included, but in 3D we set $\alpha=0$. $\phi(\boldsymbol{x},t)$ is the order-parameter field at the point $\boldsymbol{x}$ and time t [with $\phi(\boldsymbol{x},t)>0$ in the lighter phase and $\phi(\boldsymbol{x},t)<0$ in the heavier phase]. The third term on the right-hand side of Eq. (1) couples $\boldsymbol{u}$ to ϕ via the chemical potential $\mu(\boldsymbol{x},t)$, which is related to the the free energy $\mathcal{F}$ of the Cahn-Hilliard system as follows:

$$\mu = \delta\mathcal{F}[\phi]/\delta\phi(\boldsymbol{x},t), \quad (3)$$

$$\mathcal{F}[\phi] = \Lambda\int_{\mathcal{V}}\left[\frac{1}{2}|\boldsymbol{\nabla}\phi|^2 + (\phi^2-1)^2/(4\xi^2)\right]dV, \quad (4)$$

where Λ is the energy density with which the two phases mix in the interfacial regime [24], ξ sets the scale of the interface width, $\sigma = 2(2^{\frac{1}{2}})\Lambda/3\xi$ is the surface tension, γ is the mobility [29] of the binary-fluid mixture, $A = (\rho_2 - \rho_1)/(\rho_2 + \rho_1)$ is the Atwood number, and $\boldsymbol{g}$ is the acceleration due to gravity.

While solutions of the CHNS equations have been shown to be regular in the 2D case [31,32], with an equivalent body of literature associated with the CH equations alone (mainly 2D; see, e.g., Ref. [33]) a critical issue for the 3D CHNS system (1)–(4) revolves around the smoothness of the contours of ϕ packed together within the fluid interfaces. The regularity of the solutions of the 3D Navier-Stokes (NS) equations alone is in itself a major open problem [6]; a coupling of the CH and the NS equations poses additional severe difficulties. For instance, how do we know whether a slope discontinuity, such as a cusp, might develop in a finite time in arbitrarily large spatial derivatives of ϕ, thereby affecting the smoothness of these contours? Moreover, if such singularities do develop, how closely are they associated with the breakdown of regularity of the solutions of the 3D NS
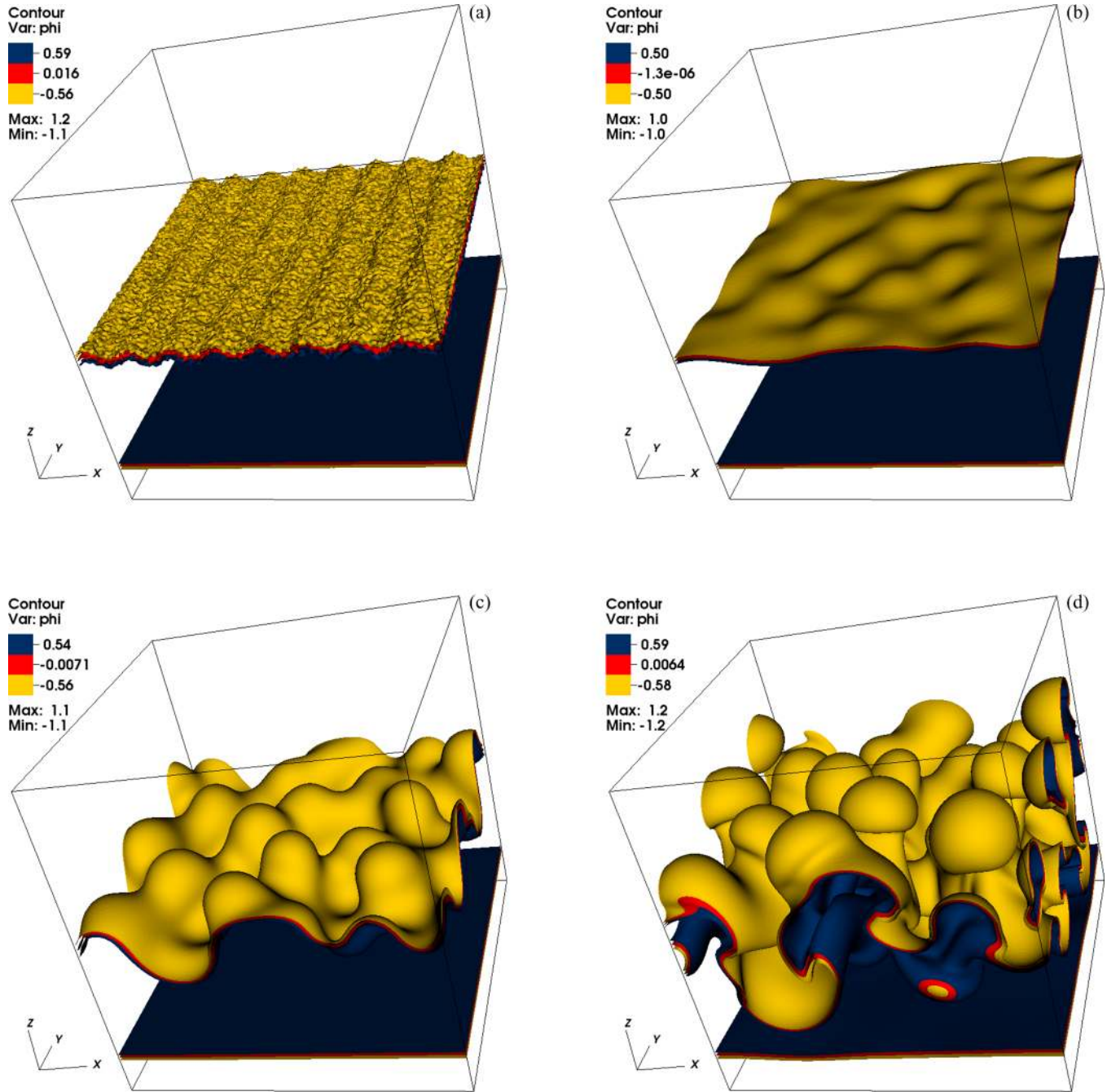
FIG. 1. Isosurface plots of the ϕ field in the 3D CHNS equations illustrating the development of the RTI with large-wavelength perturbations in 3D (DNS run T1 in Table I), with 256^3 collocation points, at times (a) $t = 1$, (b) $t = 10$, (c) $t = 25$, and (d) $t = 36$. The spatiotemporal development of this field is given in the Video RTI_Atwood=5e-1 in the Supplemental Material [53].

equations themselves? To answer such questions, we follow a strategy that is closely connected to an issue that once arose in studies of the incompressible 3D Euler equations (for a survey of the Euler literature, see Refs. [34–36]). Since the time of Leray [2,5,6] it has been known that the finiteness of $\int_{\mathcal{V}} |\boldsymbol{\omega}|^2 dV$ pointwise in time controls the regularity of solutions of the 3D incompressible NS equations, where $\boldsymbol{\omega} = \nabla \times \boldsymbol{u}$ is the vorticity. There are also a variety of alternative time integral criteria, such as the finiteness of $\int_0^T \|\boldsymbol{u}\|_\infty^2 d\tau$ or $\int_0^T (\|\boldsymbol{\omega}\|_4^2/\|\boldsymbol{\omega}\|_2) d\tau$. In addition, other conditions exist

involving the pressure [37]. In contrast, prior to 1984, it was not known what variables control the regularity of solutions of the 3D Euler equations. Beale, Kato, and Majda [38] then proved that the time integral $\int_0^{T^*} \|\boldsymbol{\omega}\|_\infty d\tau$ is the key object: if this integral becomes infinite at a finite time T^*, then solutions have lost regularity at T^* (i.e., blow-up occurs), but there exists a global solution if, for every $T > 0$, $\int_0^T \|\boldsymbol{\omega}\|_\infty d\tau < \infty$. This result is now generally referred to as the BKM theorem. Its practical value is that only one simple integral needs to be monitored numerically. It also discounts the possibility that

very large spatial derivatives of $\boldsymbol{u}$ could develop a discontinuity if the integral is finite.

The main result of this paper is that we have shown that there exists a similar result for the 3D CHNS system. It can be expressed very simply and takes its motivation from the energy $E(t)$ of the full system, which can be written as

$$E(t) = \int_{\mathcal{V}} \left[\frac{1}{2} \Lambda |\nabla \phi|^2 + \frac{\Lambda}{4\xi^2} (\phi^2 - 1)^2 + \frac{1}{2} |\boldsymbol{u}|^2 \right] dV. \quad (5)$$

Given that this can be viewed as a combination of squares of L^2 norms, it suggests a corresponding L^∞ version, which we call the *maximal energy* [39]:

$$E_\infty(t) = \frac{1}{2} \Lambda \|\nabla \phi\|_\infty^2 + \frac{\Lambda}{4\xi^2} \left(\|\phi\|_\infty^2 - 1 \right)^2 + \frac{1}{2} \|\boldsymbol{u}\|_\infty^2. \quad (6)$$

In Sec. III we prove a theorem which says that $\int_0^{T^*} E_\infty(\tau) \, d\tau$ is the key object that controls regularity of solutions of the 3D CHNS equations exactly in the same fashion as $\int_0^{T^*} \|\boldsymbol{\omega}\|_\infty \, d\tau$ does for the 3D Euler equations [38]. The proof of the theorem is technically complicated, so this is given in the Appendix A. Our numerical calculations in that section [Fig. 1 (left)] suggest that E_∞ is indeed finite.

In order to make a comparison with 3D Navier-Stokes results, we also calculate the time dependence of scaled L^{2m} norms of other fields, such as the fluid vorticity $\boldsymbol{\omega}$. The study of similar scaled norms has led to fruitful insights into the solutions of the 3D NS [40–42] and the 3D Magnetohydrodynamics (MHD) equations [43]. We find that plots of all these norms, versus time t, are ordered as a function of m (curves with different values of m do not cross); and, as $m \to \infty$, these curves approach a limit curve that can be identified as the scaled L^∞ norm.

The remainder of this paper is organized as follows: In Sec. II we discuss the numerical methods that we use to study its solutions. Section III is devoted to the statement of our E_∞ theorem and associated numerical results together with plots of the L^{2m} norms mentioned in the last paragraph. Section IV contains concluding remarks. In the Appendix we describe the details of the proof of the theorem.

II. NUMERICAL METHODS

We carry out direct numerical simulations of the 3D CHNS equations. For this we use a simulation domain that is a cubical box with sides of length 2π and periodic boundary conditions in all three directions. We use N^3 collocation points, a pseudospectral method with a $1/2$- dealiasing rule, and a second-order Adams-Bashforth method for time marching. In our DNSs we use the following two types of forcing: (a) In the first type, we use the gravity-driven Rayleigh Taylor instability (RTI) of the interface of a heavy fluid that is placed initially on top of a light fluid; this instability is of great importance in inertial-confinement fusion [44,45], astrophysical phenomena [23], and turbulent mixing, especially in oceanography [46]. (b) In the second type, we have a forcing that yields a constant energy-injection rate [47]. In our RTI studies, there is a constant gravitational field in the $\hat{z}$ direction; here we stop our DNS just before plumes of the heavy or light fluid wrap around the simulation domain in the $\hat{z}$ direction because of the periodic

TABLE I. Parameters N, A, ν, D, σ, Ch, and Gr for DNS runs T1–T3. The number of collocation points is N^3, A is the Atwood number, ν kinematic viscosity, D diffusivity, σ surface tension, Ch Cahn number, and Gr Grashof number in runs T2 and T3.

	N	A	ν	D	σ	Ch	Gr	Re_λ
T1	256	0.5	0.001 16	0.0015	0.23	0.011		
T2	128	0	0.0116	0.0015	0.23	0.011	1.2×10^7	42.23
T3	512	0	0.001 16	0.0015	0.23	0.011	1.2×10^9	300

boundary conditions. Most of the DNSs of such CHNS problems, e.g., CHNS studies of the RTI, have been motivated by experiments [48–50]. To the best of our knowledge, no studies have investigated the growth of L^{2m} norms of the quantities we have mentioned above. (For the RTI problem, some of these norms have been studied [51] by using the DNS results of Ref. [52] for the miscible, two-fluid, incompressible 3D NS equations.) It behooves us, therefore, to initiate such DNS investigations of L^{2m} norms of fields in the 3D CHNS equations.

The last-but-one term in Eq. (1) is used in our DNSs of the RTI; in these studies we set the external force $\boldsymbol{f} = 0$. We also carry out DNSs, with no gravity, but with a constant-energy-injection forcing scheme in which

$$\hat{\boldsymbol{f}} = P\Theta(k_f - k)\hat{\boldsymbol{u}}(\mathbf{k}, t)/[2E(k, t)], \quad (7)$$

where P is the energy-injection rate and Θ is the Heaviside function. For simplicity, our CHNS description of binary-fluid mixtures assumes that γ is independent of ϕ and that both components of the mixtures have the same viscosity. We keep the diffusivity $D = \gamma \Lambda / \xi^2$ constant in all our DNSs. We give the parameters for our DNS runs T1–T3 in Table I.

III. E_∞ THEOREM AND CORRESPONDING NUMERICAL RESULTS

A. E_∞ theorem

Let us consider n derivatives of both $\boldsymbol{u}$ and ϕ within L^2 norms such that for $n \geqslant 0$,

$$H_n = \int_{\mathcal{V}} |\nabla^n \boldsymbol{u}|^2 dV \quad \text{and} \quad P_n = \int_{\mathcal{V}} |\nabla^n \phi|^2 dV. \quad (8)$$

Then the CHNS equivalent of the BKM theorem [38] is the following (which we prove in the Appendix A)

Theorem 1. Consider the CHNS equations on a periodic domain $\mathcal{V} = [0, L]^3$ in three spatial dimensions. For initial data $u_0 \in H_m$, for $m > 3/2$, and $\phi_0 \in P_m$, for $m > 5/2$, suppose there exists a solution on the interval $[0, T^*)$ where T^* is the earliest time that the solution loses regularity, then

$$\int_0^{T^*} E_\infty(\tau) \, d\tau = \infty. \quad (9)$$

Conversely, there exists a global solution of the 3D CHNS equation if, for every $T > 0$,

$$\int_0^T E_\infty(\tau) \, d\tau < \infty. \quad (10)$$

The finiteness, or otherwise, of $E_\infty(t)$ is thus critical to the regularity of solutions. This needs to be tested numerically
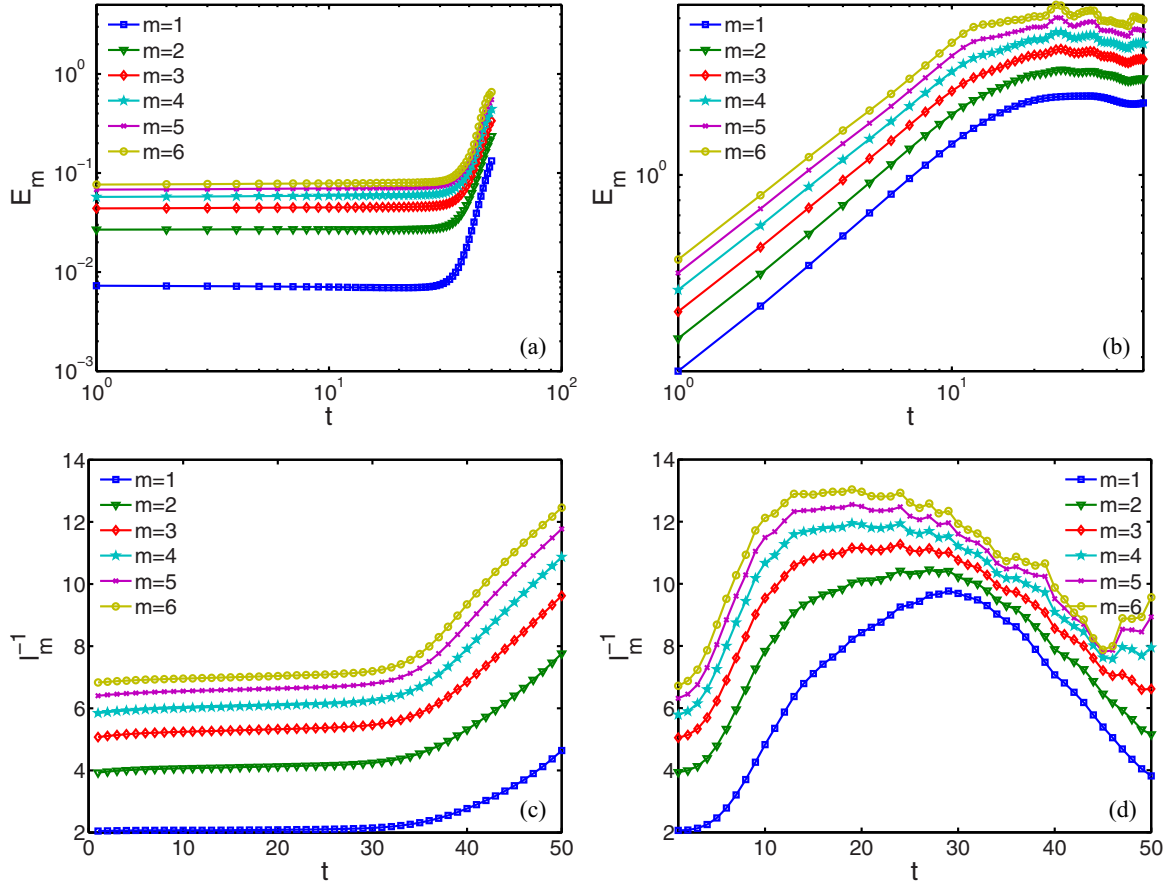
FIG. 2. Plots against time t of E_m according to Eq. (11) for $m = 1$–6 for (a) an RTI flow and (b) a flow with a constant-energy-injection forcing scheme [see Eq. (7)], with no gravity. Also, plots against time t of ℓ_m^{-1} for $m = 1$–6 for (c) an RTI flow and (d) a flow with a constant-energy-injection forcing scheme.

from different initial conditions. One way is to plot finite L^m norms of the energy, namely,

$$E_m(t) = \frac{1}{2}\Lambda \|\nabla\phi\|_m^2 + \frac{\Lambda}{4\xi^2}\left(\|\phi\|_m^2 - 1\right)^2 + \frac{1}{2}\|\boldsymbol{u}\|_m^2, \quad (11)$$

for increasing values of $m \geqslant 1$. We observe that $E_m(t)$ converges as m increases; see Figs. 2(a) and 2(b). This suggests that the integral criterion within Theorem 1 is indeed finite and thus Eq. (10) holds, leading to the regularity of these solutions, at least for the DNSs we carry out.

B. Temporal Evolution of D_m

The initial stages of the spatiotemporal development of the RTI in the 3D CHNS system is illustrated by the isosurface plots of the ϕ field in Fig. 1 (the spatiotemporal development of this field is given in the Video RTI_Atwood=5e-1 in the Supplemental Material [53]). In RTI flows, the potential energy that is stored in the initial density field is converted to kinetic energy, which initiates fluid mixing and a cascade of energy from large to small length scales; this gives rise to filamentary structures with enhanced gradients in ϕ. The nonlinearity of the binary-fluid system is responsible for this energy cascade.

For both the 3D Navier-Stokes and 3D MHD equations, a method was introduced to estimate the degree of nonlinear depletion in the vortex stretching term(s) [40–43]. It involved

the use of the following L^{2m} norms of the vorticity field $\boldsymbol{\omega} = \nabla \times \boldsymbol{u}$ defined by ($1 \leqslant m < \infty$),

$$\Omega_m(t) = \left(L^{-3}\int_{\mathcal{V}} |\boldsymbol{\omega}|^{2m} dV\right)^{1/2m}, \quad (12)$$

and also the following scaled dimensionless counterparts of Ω_m:

$$D_m(t) = \left(\varpi_0^{-1}\Omega_m\right)^{\alpha_m}, \qquad \alpha_m = \frac{2m}{4m-3}, \quad (13)$$

where $\varpi_0 = \nu L^{-2}$ is the box-size frequency of the periodic box. Although the Ω_m must obey Hölder's inequality

$$\Omega_m \leqslant \Omega_{m+1} \qquad \text{for} \qquad 1 \leqslant m < \infty, \quad (14)$$

no such natural ordering is enforced upon the D_m, because the α_m decrease with m [see Eq. (13)]. We give the plots for D_m for the RTI case in Fig. 3(a) and for the constant-energy-injection scheme in Fig. 3(d).

It was shown in Ref. [42] that there are good reasons why D_m and D_1 are such that [54]
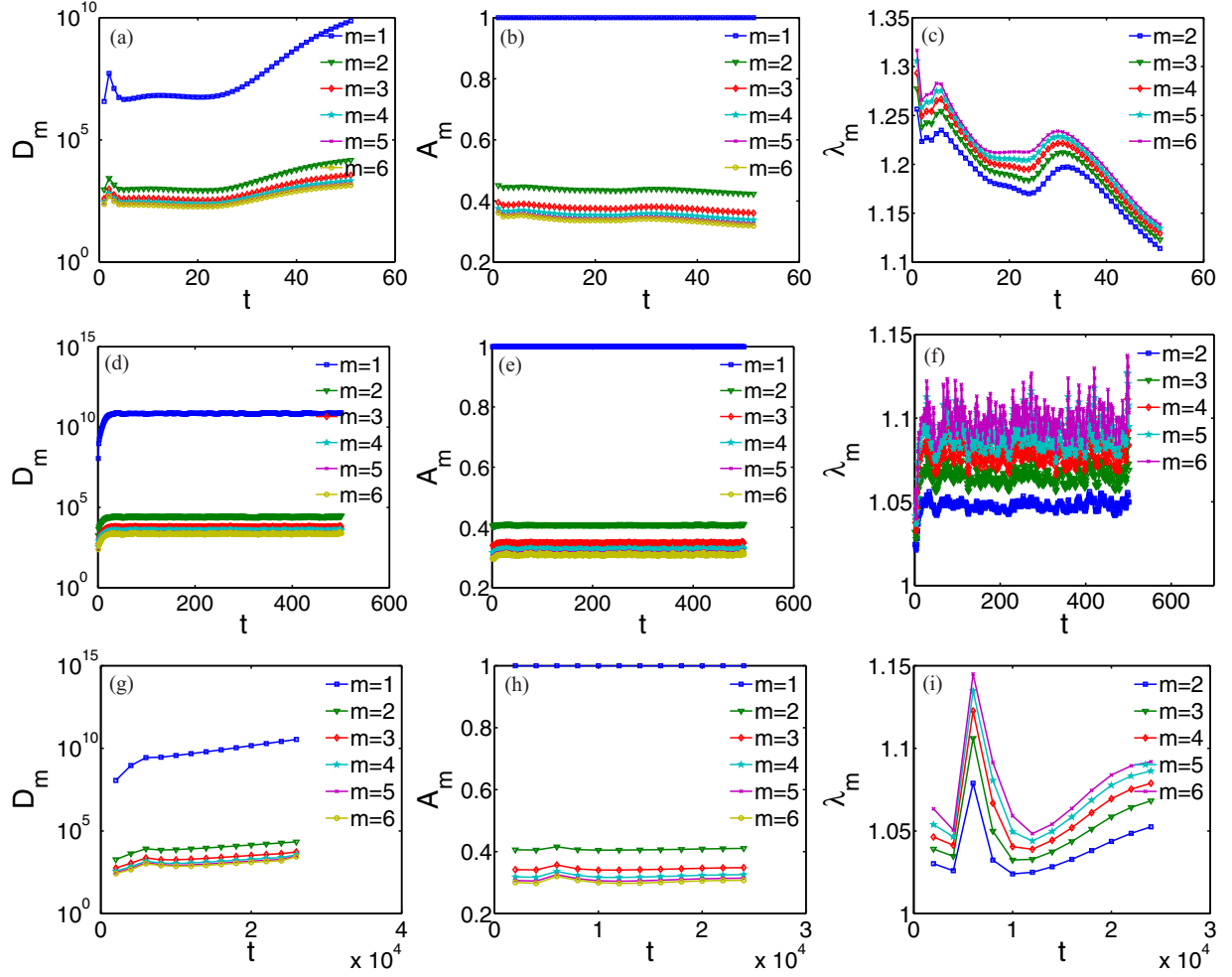
$$D_m \leqslant D_1^{A_m(t)}, \quad (15)$$

FIG. 3. Semilog (base 10) plots vs time t [with 256^3 collocation (DNS run T1)] of D_m, A_m, and $\lambda_m(t)$ for $m = 1$–6 for (a)–(c) the runs with RTI flows (DNS run T1), (d)–(f) the runs with constant-energy-injection forcing scheme (DNS run T2), and (g)–(i) for the runs with constant-energy-injection forcing scheme (DNS run T3).

with the additional relation that includes the time-dependent exponents λ_m

$$A_m(t) = \frac{\lambda_m(t)(m-1)+1}{4m-3}. \quad (16)$$

It was observed numerically [41] that the maxima of the λ_m lay in the range 1.15–1.45. For purposes of comparison between those calculations and our RTI simulation, we plot $A_m(t)$ versus t in Fig. 3(b), where

$$A_m(t) = \ln D_m / \ln D_1. \quad (17)$$

We observe that the A_m do not change significantly with t but that they depend on m. We also give the plot of $A_m(t)$ versus t for the case of constant-energy injection in Fig. 3(e). As in DNSs of the 3D Navier-Stokes equation [41], we find, for the 3D CHNS system, that D_1 lies well above the other D_m [see Figs. 3(a) and 3(c)]. We give the plots for $\lambda_m(t)$ in Fig. 3(c) (for the RTI case) and in Fig. 3(f) (for the constant-energy-injection forcing scheme). In the 3D NS case, the λ_m are related to the spectral exponents for the inertial-range, power-law form of the energy spectra [41]; the analogous relation for the 3D CHNS case is not straightforward because the power-law

ranges in such spectra depend on several parameters in the CHNS equations (see, e.g., Ref. [25]).

We also compute the temporal evolution of the L^{2m} norms of the gradients of ϕ by using the definition of the inverse length scale ℓ_m^{-1}

$$\ell_m^{-2m} = \frac{\int_{\mathcal{V}} |\boldsymbol{\nabla}\phi|^{2m} dV}{\int_{\mathcal{V}} |\phi|^{2m} dV}. \quad (18)$$

Figures 2(a)–2(d) show plots of E_m and ℓ_m^{-1} versus time t for different values of m. These are qualitatively similar to those for D_m in so far as curves for different values of m do not cross; they are ordered in m such that $\ell_m^{-1} < \ell_{m+1}^{-1}$. Furthermore, both ℓ_m^{-1} and E_m approach limiting curves as $m \to \infty$. (We mention in passing that errors increase as m increases. We present data for values of m for which we have reliable data). This clustering of the E_m suggests convergence to a finite value of E_∞.

IV. CONCLUSION

The regularity of solutions of the 3D Navier-Stokes (3D NS) equations presents formidable difficulties. It remains to this day one of the outstanding open problems in modern applied

mathematics [4]. Coupling these 3D NS equations to the 3D Cahn-Hilliard equations creates a set of 3D CHNS PDEs that governs an incompressible binary fluid, but, in so doing, creates a system where the already formidable difficulties with the 3D NS system are amplified many times over. The elegant and powerful proofs of regularity by Abels [31] and Gal and Graselli [32] in the 2D case show how much harder the coupled 2D CHNS system is to deal with than the 2D Navier-Stokes equations alone.

The main challenges in the 3D system considered here lie in the behavior of not only arbitrarily large gradients of the velocity field $\boldsymbol{u}$ but also of arbitrarily large gradients of ϕ, the order parameter. The E_∞ theorem, stated in Sec. III and proved in the Appendix A, is a conditional-regularity criterion on periodic boundary conditions that is realistically computable. The motivation for this result lies in the BKM theorem for the 3D Euler equations. Constantin and Fefferman [55] reduced the $\|\boldsymbol{\omega}\|_\infty$ within the BKM criterion to $\|\boldsymbol{\omega}\|_p$ for finite $p \geqslant 2$, but at the heavy price of introducing technically complicated, local constraints on the direction of vorticity, which are difficult to compute. Thus, the original form of the BKM theorem, with its single requirement of $\|\boldsymbol{\omega}\|_\infty$ being finite, remains the simplest regularity criterion to this day. Our E_∞ theorem is the equivalent result for the 3D CHNS system.

Our curves for E_m versus time in Fig. 2(a) suggest convergence to E_∞, with increasing values of m, thereby indicating that solutions remain regular for as long as our DNSs remain valid, even though more resolution would be desirable in the future to investigate the delicate issue of possible finite-time singularities in solutions of the 3D CHNS equations.

APPENDIX: PROOF OF THEOREM 1

In the following proof the coefficients in Eqs. (1)–(4) in the main paper are set to unity to avoid needless complication. First, we recall the definitions of H_n and P_n in Eq. (8). In addition to these we define

$$X_n = H_n + P_{n+1}. \tag{A1}$$

The proof uses the method of BKM [38], which is by contradiction. The strategy is the following: suppose there exists an interval $[0, T^*)$ on which solutions are globally regular with the earliest loss of regularity at T^*. Assume that $\int_0^{T^*} E_\infty(\tau) \, d\tau < \infty$, and then show that a consequence of this is that $X_n(T^*) < \infty$, which contradicts the statement that solutions first lose regularity at T^*. This falsifies the

assumption of the finiteness of the integral. We proceed in three steps.

Step 1. We begin with the time evolution of P_n (the dot above P_n denotes a time derivative):

$$\frac{1}{2}\dot{P}_n = -P_{n+2} + P_{n+1} + \int_{\mathcal{V}} (\nabla^n \phi) \nabla^n \Delta(\phi^3) \, dV$$
$$- \int_{\mathcal{V}} (\nabla^n \phi) \nabla^n (\boldsymbol{u} \cdot \nabla \phi) \, dV; \tag{A2}$$

and then we estimate the third term on the right as

$$\left| \int_{\mathcal{V}} (\nabla^n \phi) \nabla^n \Delta(\phi^3) \, dV \right|$$
$$\leqslant \|\nabla^n \phi\|_2 \sum_{i,j=0}^{n+2} C_{i,j}^{n+2} \|\nabla^i \phi\|_p |\nabla^j \phi\|_q \|\nabla^{n+2-i-j}\phi\|_r, \tag{A3}$$

where $1/p + 1/q + 1/r = 1/2$. Now we use a sequence of Gagliardo-Nirenberg inequalities

$$\|\nabla^i \phi\|_p \leqslant c_{n,i} \|\nabla^{n+2}\phi\|_2^{a_1} \|\phi\|_\infty^{1-a_1},$$
$$\|\nabla^j \phi\|_q \leqslant c_{n,j} \|\nabla^{n+2}\phi\|_2^{a_2} \|\phi\|_\infty^{1-a_2}, \tag{A4}$$
$$\|\nabla^n \phi\|_r \leqslant c_{n,i,j} \|\nabla^{n+2-i-j}\phi\|_2^{a_3} \|\phi\|_\infty^{1-a_3},$$

where in d dimensions

$$\frac{1}{p} = \frac{i}{d} + a_1\left(\frac{1}{2} - \frac{n+2}{d}\right),$$
$$\frac{1}{q} = \frac{j}{d} + a_2\left(\frac{1}{2} - \frac{n+2}{d}\right), \tag{A5}$$
$$\frac{1}{r} = \frac{n+2-i-j}{d} + a_3\left(\frac{1}{2} - \frac{n+2}{d}\right).$$

By summing these and using $1/p + 1/q + 1/r = 1/2$, it is seen that $a_1 + a_2 + a_3 = 1$. Thus, we have

$$\left| \int_{\mathcal{V}} (\nabla^n \phi) \nabla^{n+2}(\phi^3) \, dV \right| \leqslant c_n \|\nabla^n \phi\|_2 \|\nabla^{n+2}\phi\|_2 \|\phi\|_\infty^2$$
$$\leqslant \frac{1}{2} P_{n+2} + c_n P_n \|\phi\|_\infty^4, \tag{A6}$$

and so Eq. (A2) becomes (here and henceforth coefficients such as c_n are multiplicative constants),

$$\frac{1}{2}\dot{P}_n = -\frac{1}{2}P_{n+2} + P_{n+1} + c_n \|\phi\|_\infty^4 P_n$$
$$+ \left| \int_{\mathcal{V}} (\nabla^n \phi) \nabla^n (\boldsymbol{u} \cdot \nabla \phi) \, dV \right|. \tag{A7}$$

Estimating the last term in Eq. (A7) we have

$$\left| \int_{\mathcal{V}} (\nabla^n \phi) \nabla^n (\boldsymbol{u} \cdot \nabla \phi) \, dV \right|$$
$$= \left| -\int_{\mathcal{V}} (\nabla^{n+1} \phi) \nabla^{n-1} (\boldsymbol{u} \cdot \nabla \phi) \, dV \right|$$
$$\leqslant \|\nabla^{n+1} \phi\|_2 \sum_{i=0}^{n-1} C_i^n \|\nabla^i \boldsymbol{u}\|_p \|\nabla^{n-1-i}(\boldsymbol{\nabla}\phi)\|_q, \tag{A8}$$

where $1/p + 1/q = 1/2$. Now we use two Gagliardo-Nirenberg inequalities in d dimensions to obtain

$$\|\nabla^i \boldsymbol{u}\|_p \leqslant c \, \|\nabla^{n-1} \boldsymbol{u}\|_2^a \|\boldsymbol{u}\|_\infty^{1-a}, \qquad \text{(A9)}$$

$$\|\nabla^{n-1-i}(\boldsymbol{\nabla}\phi)\|_q \leqslant c \, \|\nabla^{n-1}(\boldsymbol{\nabla}\phi)\|_2^b \|\boldsymbol{\nabla}\phi\|_\infty^{1-b}. \quad \text{(A10)}$$

Equations (A9) and (A10) follow from

$$\frac{1}{p} = \frac{i}{d} + a\left(\frac{1}{2} - \frac{n-1}{d}\right), \qquad \text{(A11)}$$

$$\frac{1}{q} = \frac{n-1-i}{d} + b\left(\frac{1}{2} - \frac{n-1}{d}\right). \qquad \text{(A12)}$$

Because $1/p + 1/q = 1/2$ then $a + b = 1$. Thus Eq. (A3) turns into

$$\left| \int_{\mathcal{V}} (\nabla^n \phi) \nabla^n (\boldsymbol{u} \cdot \boldsymbol{\nabla}\phi) \, dV \right|$$
$$\leqslant c_n P_{n+1}^{1/2} H_{n-1}^{a/2} P_n^{b/2} \|\boldsymbol{u}\|_\infty^{1-a} \|\boldsymbol{\nabla}\phi\|_\infty^{1-b}$$
$$\leqslant P_{n+1}^{1/2} \left[c_n H_{n-1} \|\boldsymbol{\nabla}\phi\|_\infty^2\right]^{a/2} \left[P_n \|\boldsymbol{u}\|_\infty^2\right]^{b/2}$$
$$\leqslant \frac{1}{2} P_{n+1} + \frac{1}{2} a c_n H_{n-1} \|\boldsymbol{\nabla}\phi\|_\infty^2 + \frac{1}{2} b P_n \|\boldsymbol{u}\|_\infty^2, \quad \text{(A13)}$$

and Eq. (A7) becomes

$$\frac{1}{2} \dot{P}_n = -\frac{1}{2} P_{n+2} + \frac{3}{2} P_{n+1} + c_{n,1}\left(\frac{1}{2}\|\phi\|_\infty^4 + \|\boldsymbol{u}\|_\infty^2\right) P_n$$
$$+ c_{n,2} H_{n-1} \|\boldsymbol{\nabla}\phi\|_\infty^2. \qquad \text{(A14)}$$

Step 2. Now we look at H_n defined in Eq. (8) using Eq. (A15) with $\boldsymbol{f} = -\hat{z}\phi$. The easiest way is to use the 3D NS equation in the vorticity form as in Doering and Gibbon [6] to obtain the $\|\boldsymbol{u}\|_\infty^2$ term in Eq. (A16), where gradient terms have been absorbed into the pressure term, which disappears under the curl operation:

$$(\partial_t + \boldsymbol{u} \cdot \boldsymbol{\nabla})\boldsymbol{\omega} = \Delta\boldsymbol{\omega} + \boldsymbol{\omega} \cdot \boldsymbol{\nabla}\boldsymbol{u} + \boldsymbol{\nabla}\phi \times \boldsymbol{\nabla}\Delta\phi - \boldsymbol{\nabla}^\perp\phi. \tag{A15}$$

Therefore,

$$\frac{1}{2} \dot{H}_n \leqslant -\frac{1}{2} H_{n+1} + c_n \|\boldsymbol{u}\|_\infty^2 H_n$$
$$+ \left| \int_{\mathcal{V}} (\nabla^{n-1}\boldsymbol{\omega})[\nabla^{n-1}(\boldsymbol{\nabla}\phi \times \Delta\boldsymbol{\nabla}\phi)] \, dV \right|$$
$$+ \left| \int_{\mathcal{V}} (\nabla^{n-1}\boldsymbol{\omega})[\nabla^{n-1}\boldsymbol{\nabla}^\perp\phi] \, dV \right|. \qquad \text{(A16)}$$

Beginning with the third term on the right-hand side of Eq. (A16), we obtain

$$\left| \int_{\mathcal{V}} (\nabla^{n-1}\boldsymbol{\omega}) \nabla^{n-1}(\boldsymbol{\nabla}\phi \times \Delta\boldsymbol{\nabla}\phi) \, dV \right|$$
$$\leqslant \|\nabla^{n-1}\boldsymbol{\omega}\|_2 \sum_{i=0}^{n-1} C_i^n \|\nabla^i(\boldsymbol{\nabla}\phi)\|_r \|\nabla^{n+1-i}(\boldsymbol{\nabla}\phi)\|_s. \quad \text{(A17)}$$

Then, by using a Gagliardo-Nirenberg inequality,

$$\|\nabla^i(\boldsymbol{\nabla}\phi)\|_r \leqslant c \, \|\nabla^{n+1}(\boldsymbol{\nabla}\phi)\|_2^a \|\boldsymbol{\nabla}\phi\|_\infty^{1-a}, \qquad \text{(A18)}$$

$$\|\nabla^{n+1-i}(\boldsymbol{\nabla}\phi)\|_s \leqslant c \, \|\nabla^{n+1}(\boldsymbol{\nabla}\phi)\|_2^b \|\boldsymbol{\nabla}\phi\|_\infty^{1-b}, \quad \text{(A19)}$$

where $1/r + 1/s = 1/2$ and where

$$\frac{1}{r} = \frac{i}{d} + a\left(\frac{1}{2} - \frac{n+1}{d}\right) \qquad \text{(A20)}$$

$$\frac{1}{s} = \frac{n+1-i}{d} + b\left(\frac{1}{2} - \frac{n+1}{d}\right), \qquad \text{(A21)}$$

we find that $a + b = 1$. This yields

$$\left| \int_{\mathcal{V}} (\nabla^{n-1}\boldsymbol{\omega}) \nabla^{n-1}(\boldsymbol{\nabla}\phi \times \Delta\boldsymbol{\nabla}\phi) \, dV \right|$$
$$\leqslant c_n H_n^{1/2} P_{n+2}^{1/2} \|\boldsymbol{\nabla}\phi\|_\infty$$
$$\leqslant P_{n+2} + \frac{1}{4} c_n H_n \|\boldsymbol{\nabla}\phi\|_\infty^2. \qquad \text{(A22)}$$

The last term on the right-hand side of Eq. (A16) is easily handled. Altogether we find

$$\frac{1}{2} \dot{H}_n \leqslant -\frac{1}{2} H_{n+1} + P_{n+2} + c_{n,3}\left(\|\boldsymbol{u}\|_\infty^2 + \|\boldsymbol{\nabla}\phi\|_\infty^2\right) H_n$$
$$+ \frac{1}{2} H_n + \frac{1}{2} P_n. \qquad \text{(A23)}$$

Step 3. Finally, by noting that $X_n = P_{n+1} + H_n$, we use Eq. (A6) with $n \to n+1$ to obtain

$$\frac{1}{2} \dot{X}_n \leqslant -\frac{1}{2} P_{n+3} + \frac{3}{2} P_{n+2} + c_{n,1}\left(\frac{1}{2}\|\phi\|_\infty^4 + \|\boldsymbol{u}\|_\infty^2\right) P_{n+1}$$
$$+ c_{n,2} H_n \|\boldsymbol{\nabla}\phi\|_\infty^2 - \frac{1}{2} H_{n+1} + P_{n+2}$$
$$+ c_{n,3}\left(\|\boldsymbol{u}\|_\infty^2 + \|\boldsymbol{\nabla}\phi\|_\infty^2\right) H_n + \frac{1}{2} H_n + \frac{1}{2} P_n$$
$$\leqslant -\frac{1}{2} P_{n+3} - \frac{1}{2} H_{n+1} + \frac{5}{2} P_{n+2}$$
$$+ c_{n,4}\left(\frac{1}{2}\|\phi\|_\infty^4 + \|\boldsymbol{u}\|_\infty^2 + \|\boldsymbol{\nabla}\phi\|_\infty^2\right) X_n$$
$$+ \frac{1}{2} H_n + \frac{1}{2} P_n. \qquad \text{(A24)}$$

By using $P_{n+2} \leqslant P_{n+3}^{1/2} P_{n+1}^{1/2} \leqslant (\varepsilon/2)P_{n+3} + (1/2\varepsilon)P_{n+1}$, with ε chosen as $\varepsilon = \frac{1}{5}$, we have (with $P_n \leqslant P_{n+1}$)

$$\frac{1}{2} \dot{X}_n \leqslant -\frac{1}{4} P_{n+3} - \frac{1}{2} H_{n+1}$$
$$+ c_{n,4}\left(\|\boldsymbol{\nabla}\phi\|_\infty^2 + \frac{1}{2}\|\phi\|_\infty^4 + \|\boldsymbol{u}\|_\infty^2 + \frac{1}{2}\right) X_n. \qquad \text{(A25)}$$

We note that ϕ is a mean-zero function on a unit periodic domain, so $\|\phi\|_\infty \leqslant \|\boldsymbol{\nabla}\phi\|_\infty$. Then we can write

$$c_{n,4}\left(\|\boldsymbol{\nabla}\phi\|_\infty^2 + \frac{1}{2}\|\phi\|_\infty^4 + \|\boldsymbol{u}\|_\infty^2 + \frac{1}{2}\right)$$
$$= c_{n,4}\left(\|\boldsymbol{\nabla}\phi\|_\infty^2 + \frac{1}{2}\left(\|\phi\|_\infty^2 - 1\right)^2 + \|\boldsymbol{u}\|_\infty^2 + \|\phi\|_\infty^2\right)$$
$$\leqslant 2c_{n,4}\left(\|\boldsymbol{\nabla}\phi\|_\infty^2 + \frac{1}{2}\left(\|\phi\|_\infty^2 - 1\right)^2 + \|\boldsymbol{u}\|_\infty^2\right). \quad \text{(A26)}$$

By dropping the negative terms, Eq. (A25) turns into

$$\frac{1}{4} \dot{X}_n \leqslant c_{n,4} E_\infty X_n, \qquad \text{(A27)}$$

where E_∞ is defined in Eq. (6). By integrating over $[0, T^*]$, we obtain

$$X_n(T^*) \leqslant c_{n,5} X_n(0) \exp \int_0^{T^*} E_\infty(\tau)\, d\tau. \qquad (A28)$$

The assumption that the time integral is finite implies that $X_n(T^*) < \infty$, which contradicts the statement in the theorem that solutions first lose regularity at T^*. ∎

[1] C. L. M. H. Navier, Mem. Acad. Sci. Inst. France **6**, 389 (1822); G. G. Stokes, *Mathematical and Physical Papers*, Vol. 1 (Cambridge University, Cambridge, UK, 1880).

[2] J. Leray, Acta Math. **63**, 193 (1934).

[3] G. K. Batchelor, *An Introduction to Fluid Mechanics* (Cambridge University, Cambridge, UK, 2000).

[4] P. Constantin, C. Fefferman, and A. J. Majda, Comm. PDEs **21**, 3 (1996).

[5] C. Foias, O. Manley, R. Rosa, and R. Temam, *Navier-Stokes Equations and Turbulence* (Cambridge University, Cambridge, UK, 2001).

[6] C. R. Doering and J. D. Gibbon, *Applied Analysis of the Navier-Stokes Equations* (Cambridge University, Cambridge, UK, 2004).

[7] J. W. Cahn and J. E. Hilliard, J. Chem. Phys **28**, 258 (1958).

[8] P. M. Chaikin and T. C. Lubensky, *Principles of Condensed Matter Physics* (Cambridge University, Cambridge, UK, reprint edition 2000).

[9] P. C. Hohenberg and B. I. Halperin, Rev. Mod. Phys. **49**, 435 (1977).

[10] I. M. Lifshitz and V. V. Slyozov, J. Phys. Chem. Solids **19**, 35 (1959); H. Furukawa, Phys. Rev. A **31**, 1103 (1985); E. D. Siggia, *ibid.* **20**, 595 (1979).

[11] J. D. Gunton, M. San Miguel, and P. S. Sahni, in *Phase Transitions and Critical Phenomena*, edited by C. Domb and J. L. Lebowitz, Vol. 8 (Academic, London, 1983).

[12] A. J. Bray, Adv. Phys. **43**, 357 (1994).

[13] S. Puri, in *Kinetics of Phase Transitions*, edited by S. Puri and V. Wadhawan, Vol. 6 (CRC Press, Boca Raton, FL, 2009), p. 437.

[14] J. Lothe and G. M. Pound, J. Chem. Phys. **36**, 2080 (1962).

[15] A. Onuki, *Phase Transition Dynamics* (Cambridge University, Cambridge, UK, 2002).

[16] V. E. Badalassi, H. D. Ceniceros, and S. Banerjee, J. Comput. Phys. **190**, 371 (2003).

[17] P. Perlekar, R. Benzi, H. J. H. Clercx, D. R. Nelson, and F. Toschi, Phys. Rev. Lett. **112**, 014502 (2014).

[18] J. W. Cahn, Acta Metall. **9**, 795 (1961).

[19] S. Berti, G. Boffetta, M. Cencini and A. Vulpiani, Phys. Rev. Lett. **95**, 224501 (2005); A. J. Wagner and J. M. Yeomans, *ibid.* **80**, 1429 (1998); V. M. Kendon, Phys. Rev. E **61**, R6071(R) (2000); V. M. Kendon, M. E. Cates, I. Pagonabarraga, J. C. Desplat, and P. Blandon, J. Fluid Mech. **440**, 147 (2001).

[20] G. Boffetta and R. E. Ecke, Annu. Rev Fluid Mech. **44**, 427 (2012); R. Pandit, P. Perlekar, and S. S. Ray, Pramana J. Phys. **73**, 157 (2009).

[21] A. Castro, D. Cordoba, Ch. Fefferman, F. Gancedo and M. López-Fernández, Ann. Math. **175**, 909 (2012).

[22] A. Castro, D. Cordoba, Ch. Fefferman, and F. Gancedo, Arch. Ration. Mech. Anal. **208**, 805 (2013).

[23] W. H. Cabot and A. W. Cook, Nat. Phys. **2**, 562 (2006).

[24] A. Celani, A. Mazzino, P. Muratore–Ginanneschi, and L. Vozella, J. Fluid Mech. **622**, 115 (2009).

[25] N. Pal, P. Perlekar, A. Gupta, and R. Pandit, Phys. Rev. E **93**, 063115 (2016).

[26] O. Shardt, S. K. Mitra, and J. J. Derksen, Langmuir **30**, 14416 (2014).

[27] A. Gupta and M. Sbragaglia, Phys. Rev. E **90**, 023305 (2014).

[28] L. Scarbolo and A. Soldati, J. Turb. **14**, 27 (2013).

[29] P. Yue, J. J. Feng, C. Liu, and J. Shen, J. Fluid Mech. **515**, 293 (2004).

[30] L. Scarbolo, D. Molin, and A. Soldati, APS Div. Fluid Dynamics Meeting Abstracts. **1**, 4002 (2011).

[31] H. Abels, in *Proceedings of the Conference on Nonlocal and Abstract Parabolic Equations and Their Applications*, Vol. 86 (Banach Center Publications, Warsaw, 2009).

[32] C. G. Gal and M. Graselli, Ann. Inst. Henri Poincaré (C) Anal. Nonlin. **27**, 401 (2010).

[33] C. M. Elliott and Z. Songmu, Arch. Rat. Mech. Anal. **96**, 339 (1986).

[34] A. J. Majda and A. Bertozzi, *Vorticity and Incompressible Flow*, Cambridge Texts in Applied Mathematics, No. 27 (Cambridge University, Cambridge, UK, 2001).

[35] J. D. Gibbon, Physica D **237**, 1894 (2008).

[36] C. Bardos and E. S. Titi, Russ. Math. Surv. **62**, 409 (2007).

[37] C. V. Tran and X. Yu, Nonlinearity **29**, 2990 (2016).

[38] J. T. Beale, T. Kato, and A. J. Majda, Commun. Math. Phys. **94**, 61 (1984).

[39] The L^∞ norm of a function is also referred to as the sup- or maximum norm.

[40] D. A. Donzis, J. D. Gibbon, A. Gupta, R. M. Kerr, R. Pandit, and D. Vincenzi, J. Fluid Mech. **732**, 316 (2013).

[41] J. D. Gibbon, D. A. Donzis, A. Gupta, R. M. Kerr, R. Pandit and D. Vincenzi, Nonlinearity **27**, 1 (2014).

[42] J. D. Gibbon, IMA J. Appl. Math. **81**, 308 (2015).

[43] J. D. Gibbon, A. Gupta, G. Krstulovic, R. Pandit, H. Politano, Y. Ponty, A. Pouquet, G. Sahoo, and J. Stawarz, Phys. Rev. E **93**, 043104 (2016).

[44] R. D. Petrasso, Nat. Phys. **367**, 217 (1994).

[45] R. P. Taleyarkhan, Science **295**, 1868 (2002).

[46] W. Munk and C. Wunsch, Deep-Sea Res. I **45**, 1977 (1998).

[47] A. Bhatnagar, A. Gupta, D. Mitra, P. Perlekar, and R. Pandit, arXiv:1412.2686.

[48] J. T. Waddell, C. E. Niederhaus, and J. W. Jacobs, Phys. Fluids **13**, 1263 (2001).

[49] P. Ramaprabhu, G. Dimonte, Y. N. Young, A. C. Calder, and B. Fryxell, Phys. Rev. E **74**, 066308 (2006).

[50] S. B. Dalziel *et al.*, Phys. Fluids **20**, 065106 (2008).

[51] P. Rao, C. P. Caulfield, and J. D. Gibbon, arXiv:1601.03445.

[52] D. Livescu, Phil. Trans. R. Soc. A **371**, 20120185 (2013).

[53] See Supplemental Material at http://link.aps.org/supplemental/10.1103/PhysRevE.94.063103 for the video sequence showing isosurface plots of the ϕ field for parameters of our simulations T1. Here kinematic viscosity $= 1.167 \times 10^{-3}$. For this video, we use 10 frames/s with each frame separated from the succeeding frame by $200\delta t$, where $\delta t = 10^{-3}$.

[54] In [42] a set of multiplicative positive constants C_m were included.

[55] P. Constantin and C. Fefferman, Indiana Univ. Math. J. **42**, 775 (1993).